Hindawi
Journal of Chemistry
Volume 2023, Article ID 4550047, 12 pages
https://doi.org/10.1155/2023/4550047

Research Article

Volatile Components' Variation Analysis on Ginseng Stems and Leaves at Different Growth Ages by HS-SPME-GC-MS

Hui-E. Zhang,[1] **Guang Li**,[1] **JianFeng Hou**,[2] **YanYan Han**,[1] **Ping Ye**,[1] **ChangBao Chen**,[1] **XiaoHong Xu**,[1] **and EnPeng Wang**[1]

[1]*Jilin Ginseng Academy, Changchun University of Chinese Medicine, Changchun 130117, Jilin, China*
[2]*Shiqi Biological R&D Centre (Suzhou Industrial Park) Co. Ltd., Suzhou 215125, Jiangsu, China*

Correspondence should be addressed to XiaoHong Xu; 740761229@qq.com and EnPeng Wang; wangep@ccucm.edu.cn

Received 16 October 2022; Revised 2 December 2022; Accepted 11 May 2023; Published 25 May 2023

Academic Editor: Serkan Selli

Panax ginseng is a famous valuable folk herb, the price of which particularly depends on its cultivation age. Since the classical chemical analysis usually needs to destroy the plants which is not suitable for the old wild ginseng due to the huge cost, in the current study, we employed the headspace solid-phase microextraction (HS-SPME) GC-MS methodology which has the advantage of time-saving, nondestructive, and green to analyze the growth age of ginseng (roots) via determining the volatile components of ginseng stem and leaves (GSLs) combined with metabolic profiles way. 100 mg of finely ground GSL samples (3–7 years) were extracted by a 65 μm PDMS-DVB fiber in the headspace and then analyzed within 20 mins. The content assay of total saponins, crude polysaccharides, and total protein was also included. As a result of GC-MS-based profiling, the orthogonal partial least-squares discriminant analysis' (OPLS-DA) score plots showed excellent classification of four comparison groups (the 3- and 4-, 3-and 5-, 3- and 6-, and 3- and 7-year-old GSL) with 100% discrimination rate, respectively. 263 common differential variables were gained referring to the VIP and P values. 32 volatile metabolites were identified and showed good age discrimination capacities with an area under the curve (AUC) value of more than 0.8 by the receiver operating characteristic (ROC) analysis. Remarkably, there was one volatile component of sesquiterpenes, 1-cyclohexene-1-carboxaldehyde, 2, 6, 6-trimethyl-, which showed an excellent prediction with the AUC value of 1.0 among all the four compared groups, which could be the potential biomarker to distinguish all the four compared groups. The total contents of different growth ages of components of ginseng stems and leaves were distinct. The contents of total protein (4.80 ± 0.27%) and crude polysaccharide (24.15 ± 0.89%) in the 4th year of GSLs were the highest among the five cultivation years. The content of total saponins (4.66 ± 0.38%) in the 5th year of GSLs was the highest. These results could provide a novel reference for the GSLs' harvest and application periods. Moreover, the current study could also supply a promising way to set up a nondestructive, in situ, and green approach to discriminate the growth age of Panax ginseng rapidly without digging the roots out instead of detecting the VOCs of GSLs.

1. Introduction

Panax ginseng C. A. Mey is the root and rhizome of the Araliaceae species ginseng, which originated from the Far East, mainly distributed in China, the Korean Peninsula, Japan, and eastern Russia in eastern Asia, with China as the main producing area, among which the Changbai Mountain in Jilin province has the highest yield [1–3]. It is a perennial crop, and 3–7-year-old ginseng is used in many medicines [4]. Compared to ginseng roots, many studies of ginsenosides have focused on the roots and rhizomes of ginseng because the aerial parts including stems and leaves are usually discarded. However, some recent studies have focused on the pharmacological effects of compounds in ginseng stems and leaves (GSLs) harvested annually, showing that the ginsenoside components in GSLs are related to the rhizome and root of ginseng [5]. In addition, GSLs have the advantages of being rich in resources, large in annual output, inexpensive, and easy to obtain [6]. So it has development potential and commercial value. As the main active ingredient of ginseng, ginsenoside has various therapeutic effects, such as enhancing immunity, anticancer,

lowering blood sugar, anti-inflammatory, antioxidation, antiapoptosis [7], and protecting the central nervous system [8].

Moreover, polysaccharides and proteins are the basic substances for plant growth and development [9]. They are involved in a series of physiological activities such as seed germination and development, root and leaf differentiation, fruit ripening, embryo formation, and senescence [10]. Terpenoids are a kind of natural hydrocarbon compound that widely exists in plants. There are more than 7000 kinds of sesquiterpenes, which are the largest kind of terpenoids and play an important role in plant growth and development [11]. For example, the plant hormone abscisic acid is formed from sesquiterpenes degraded by carotenoid precursors [12]. The accumulation of patchouli oil (mainly composed of sesquiterpene patchouli alcohol) gradually increased with the plant's age [13].

Several studies have reported that the pharmacological components and effects of ginseng change with age [14, 15]. Similarly, the content of ginsenosides in GSL can be different depending on the growth age. Qu et al. [16] have reported that the contents of ginsenosides Rg1, Re, Rf, Rb1, Rc, and Rb2 tend to increase with growing age. As the growth age of ginseng can hardly be determined by physical appearance, a reliable method to discriminate the growth age of ginseng is required. A study shows that ginseng of different growth ages can be successfully differentiated by the metabolomics approach [17]. However, to make better use of ginseng resources and be dedicated to establishing a nondestructive pathway to achieve in situ, rapid detection, it is necessary to study the variation of GSLs' characteristics under different growth years. Headspace solid-phase microextraction (SPME) is a relatively new volatile extraction technique. Furthermore, SPME allows the enrichment of volatiles in gas or liquid samples by fused silica fibers followed by subsequent desorption of these less volatile analytes [18, 19]. This technique is suitable for sample processing and analysis of volatile and semivolatile organic compounds. Compared to other commonly used volatile substances acquisition technologies, HS-SPME has the advantages of simplicity, solvent-free, and high sensitivity. It integrates sampling, extraction, concentration, and sample injection. After enrichment, it can be directly combined with gas chromatography-mass spectrometry (GC-MS), high-performance liquid chromatography (HPLC), capillary electrophoresis (CE), and other methods [20]. Besides the advantages, it also has drawbacks, including the limited mechanical robustness of the fiber and the rather small sorption phase volume of the commercially available fibers [21]. In addition, GC-MS is a highly sensitive and comprehensive analytical tool for volatile and semivolatile organic compounds in mixture samples. A reference library of GC-MS has been established for many primary metabolites [22]. By using the method, we tried to obtain a complementary profile to discriminate volatile components by checking the overall profile difference of primary and secondary metabolites in ginseng stems and leaves [23, 24]. Metabolomics can identify changes in metabolic profiles [25]. We speculate that the volatile components and metabolic profiles of GSLs at different growth ages may change in a predictable manner.

This study was based on 3–7-year-old GSLs to explore the differences of saponins, crude polysaccharide, total protein, and volatile content in GSLs. Trying to discover their correlation and variation, and to provide a more scientific basis for identifying the GSLs and other Chinese herbal medicine of different growth years, it also provides a reference for the reasonable collection time and quality control of ginseng.

2. Materials and Methods

2.1. Chemicals and Materials. The alkanes (C_8–C_{30}) were purchased from Alfa Aesar (USA); methanol, anhydrous ethanol, concentrated sulfuric acid, and acetic acid (all analytical purity >98%) were purchased from Beijing Chemical Plant; vanillin was purchased from Shanghai Yongyi Biotechnology Co., Ltd. Reference standards for ginsenoside Re were obtained from the Department of Organic Chemistry, Jilin University. Bovine serum albumin was purchased from the National Institute of Metrology, China, glucose standard was purchased from Beijing Putian Tongchuang Biotechnology Co., Ltd. 96-well plates were purchased from Costar, USA, polydimethylsiloxane-divinylbenzene (PDMS-DVB/65 μm) and 12 mL headspace extraction bottles were purchased from Supelco, USA.

TRACE 1310 GC-triple quadrupole MS gas chromatography-tandem mass spectrometry was purchased from Thermo Fisher, USA, P-VP-III-40 ultrapure water machine for laboratory was purchased from Sichuan Walter Technology Development Co., Ltd., centrifuge 5804R was purchased from Eppendorf, USA; XP205 precision analytical balance was purchased from Metler, Switzerland, H-8 digital display constant temperature water bath pot was purchased from Changzhou Zhiborui Instrument Manufacturing Co., Ltd., infinite M200 PRO microplate reader (Tecan, Switzerland), and A11B S025 Crusher was purchased from Germany IKA Equipment Co., Ltd.

2.2. Plant Materials. Ginseng stems and leaves were collected in Wanliang Town, Fusong County, Jilin Province, which is a major production area in the northern-east region. Ginseng stems and leaves of 3-, 4-, 5-, 6-, and 7-year-olds were harvested in 2019 (September).

2.3. Sample Preparation. 3–7-year-old ginseng stem and leaf samples were washed and dried in a drying oven at 40°C for 48 h, then weighed. The stems and leaves were ground to 10 mm or less using a superfine grinding machine (XDW-6B, Jinan, China). Then, 100 mg of finely ground GSLs and 10 mg NaCl (GR) were transferred into a 12 mL headspace vial refrigerator for spare.

2.4. Contents of Total Saponins in GSLs. The total saponin content was determined according to Bradford's method with BSA as a standard [26].

2.5. Contents of Crude Polysaccharide in GSLs. The total polysaccharide content was evaluated by a phenol sulfuric acid method using glucose as a reference [27].

2.6. Contents of Total Protein in GSLs. The total protein content was determined according to the Coomassie brilliant blue G-250 colorimetric method [28].

2.7. Headspace Solid-Phase Microextraction (HS-SPME). Ginseng stem and leaf powders were weighed (100 mg), placed in a 12 mL headspace flask, and sealed hermetically with a Teflon cap. The sample was immersed in a constant temperature water bath at 70°C for 30 minutes prior to the analysis. Then, the 65 μm PDMS-DVB fiber (Supelco, USA) was exposed to the solid-phase microextraction fiber 2 cm above the sample for 45 minutes to extract the VOCs. Then, the fiber was conditioned according to the instructions of the supplier [29, 30]. The retention index was determined by n-alkanes (C_8–C_{30}). The QC samples were obtained by equally mixing all the samples analyzed. The QC samples were processed according to the abovementioned method, and one needle of QC samples was injected every 6–8 samples to ensure the stability and reproducibility of the experimental system for validating the stability and reproducibility of the GC-MS system. Each sample was measured three times in parallel.

2.8. Gas Chromatography-Mass Spectrometry (GC-MS) Analysis. Gas chromatography with a time-of-flight mass spectrometry system consisting of a TRACE 1310 (Waltham, MA, USA) with a fused silica capillary column DB-5MS (30 m × 0.25 mm, 0.25 μm; Agilent, USA) was employed. The injection was conducted in splitless mode at 250°C. The condition of the program raising temperature was performed as follows: 50°C lasted for 0–2 min, then increased to 200°C at a rate of 10°C/min and held for 10 min, and then increased to 280°C at a rate of 5°C/min. Ultrahigh purity (99.9995%) helium was used as a carrier gas with an average linear velocity of 1.0 mL/min and a split ratio of 1 : 30. The transfer line temperature of mass spectrometry was 280°C, an ion source of 280°C, and the electron impact ionization was tuned to 70 eV with mass ranges from 50 to 500 m/z.

2.9. Data Processing and Statistical Analysis. All majority peaks, being above the analytical noise and representing 95% of the chromatogram peaks [31], were integrated using MassHunter Qualitative Analysis B.06.00 software (Agilent Technologies). This software allows for the deconvolution of the chromatograms by separating the coeluted compounds. The identification of the volatile compounds was performed by comparing the retention indices (RI) relative to n-alkanes (C_8–C_{20}), run under identical conditions for GC-MS, with those of the compounds in the National Institute of Standard and Technologies (NIST) online library (http://webbook.nist.gov/chemistry/casser.html), by comparing the mass spectra of the compounds with those of the compounds referenced in the NIST databases (RSI > 800) and by comparing the retention times and mass spectra of the compounds with those of the available standards [32]. For statistical analysis, peak area values of the total ion chromatograms were measured with MassHunter and transferred to Excel (Microsoft Excel 2010). The data obtained after the analysis of the GSLs of different harvest periods were subjected to PCA using SIMCA-P software (v15.0, Umetrics, Sweden).

The Microsoft Excel 2010 software was conducted for statistical analysis and charting of data. The data were expressed as mean values ± standard deviation with six replicated measurements. The analysis of variance (ANOVA) was used in the statistical analysis of the data and was computed in SPSS Statistics 21.0 (SPSS Inc., Shanghai, China) software, and a probability value of $P < 0.05$ was considered to represent a statistically significant difference among mean values. The heat map and receiver operating characteristic (ROC) analysis were conducted by MetaboAnalyst 5.0 platform (https://www.metaboanalyst.ca/).

3. Results and Discussion

3.1. Determination of Total Saponins in GSLs. 5 year old ginseng plants are usually regarded as mature enough to harvest for medicinal utilization [33]. In this study, the change of total saponin content in GSLs with growth years was GSL5 (4.66 ± 0.38%) > GSL3 (4.61 ± 0.53%) > GSL6 (4.35 ± 0.25%) > GSL4 (4.31 ± 0.23%) > GSL7 (2.65 ± 0.28%), and the content of total saponins in GSLs of GSL5 was the highest (Figure 1(a)).

3.2. Determination of Crude Polysaccharide Content in GSLs. The crude polysaccharide content of GSLs changed irregularly with the increase of years. The change rule is GSL4 (24.15 ± 0.89%) > GSL7 (22.30 ± 0.83%) > GSL6 (13.72 ± 0.93%) > GSL5 (12.99 ± 0.78%) > GSL3 (12.59 ± 0.38%). The crude polysaccharide contents varied significantly ($P < 0.05$) among GSL3-GSL7 samples (Figure 1(b)).

3.3. Determination of Total Protein Content in GSLs. The total protein content of GSLs varied with the growth years was GSL4 (4.80 ± 0.27%) > GSL6 (4.34 ± 0.19%) > GSL3 (4.33 ± 0.08%) > GSL5 (3.74 ± 0.18%) > GSL7 (2.10 ± 0.16%), and the total protein content was the highest in GSL4. By comparison, the results showed that the total protein content of ginseng stems and leaves in different years was statistically significant (Figure 1(c)).

3.4. Multivariate Statistical Analysis of VOCs in GSLs of Various Growth Times. To compare the changes in these volatile metabolites between ginseng stem and leaf samples of different growth ages, the PCA and OPLS-DA methods were employed. PCA is a multivariate statistical analysis method that can reduce the dimensionality of the data while information on the original data is still retained by using several variables to select a smaller number of important variables by linearly transforming the data. Figure 2 shows

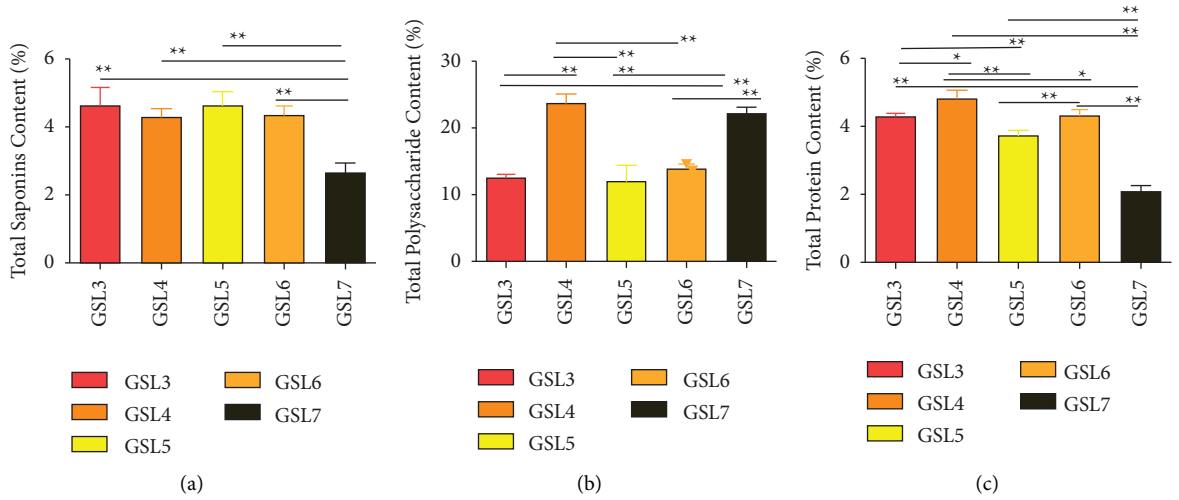

Figure 1: The content of total saponins (a), crude polysaccharide (b), and total protein (c) in GSLs of various ages. GSL3, 4, 5, 6, and 7 represent GSLs for 3-, 4-, 5-, 6-, and 7-year-olds; the symbols $*$ and $**$ are used to indicate statistical significance with $P < 0.05$ and $P < 0.01$, respectively.

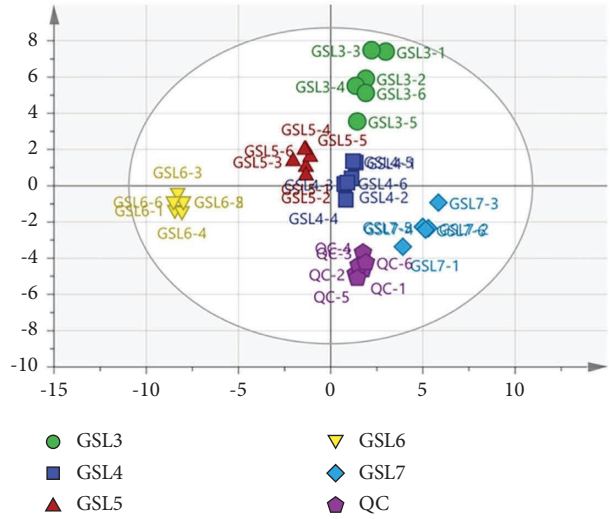

Figure 2: Score plots of principal component analysis (PCA) from metabolite profiling data of GC-MS of GSL samples of various harvest times and QC samples.

the PCA score plot of the major principal components. All samples fell outside Hotelling's T2 tolerance ellipse with 95% confidence, suggesting that no outlier was observed [34, 35]. QC samples were clustered closely, indicating that the method was stable and reproducible.

3.5. Discovery and Identification of Biomarkers for Volatile Components in GSLs in Different Harvest Periods. A supervised OPLS-DA model was used to identify the variables responsible for the classification [36]. In the OPLS-DA score plot (Figure 3), the results of group separation were consistent with the PCA score plot (Figure 2), and each group was more closely clustered. A permutation test ($n = 200$) was applied to estimate the robustness and predictive ability of the model indicating the robustness of the model and showing a low risk of overfitting. The results demonstrated that the model was stable and reproducible. Critical volatile metabolites were selected based on the two following conditions: variable importance in projection (VIP) values >1.0 and P values <0.05. The marker differential components of GSL3-GSL7 were screened, which are presented in Figure 4. 415 variables were screened out in GSL3 and GSL4. 501 variables were screened out from GSL3 and GSL5 ratios. 701 variables were screened out by GSL3 and GSL6 comparison. 629 variables were screened out from GSL3 and GSL7. Then, the Origin software was employed to demonstrate the common variables, 263 were shown to be the common variables among the 3–7 old consecutive cultivation years.

All the 263 common differential metabolites were matched with the NIST online library, in-house library, and references, and then compared to the retention indices (RI)

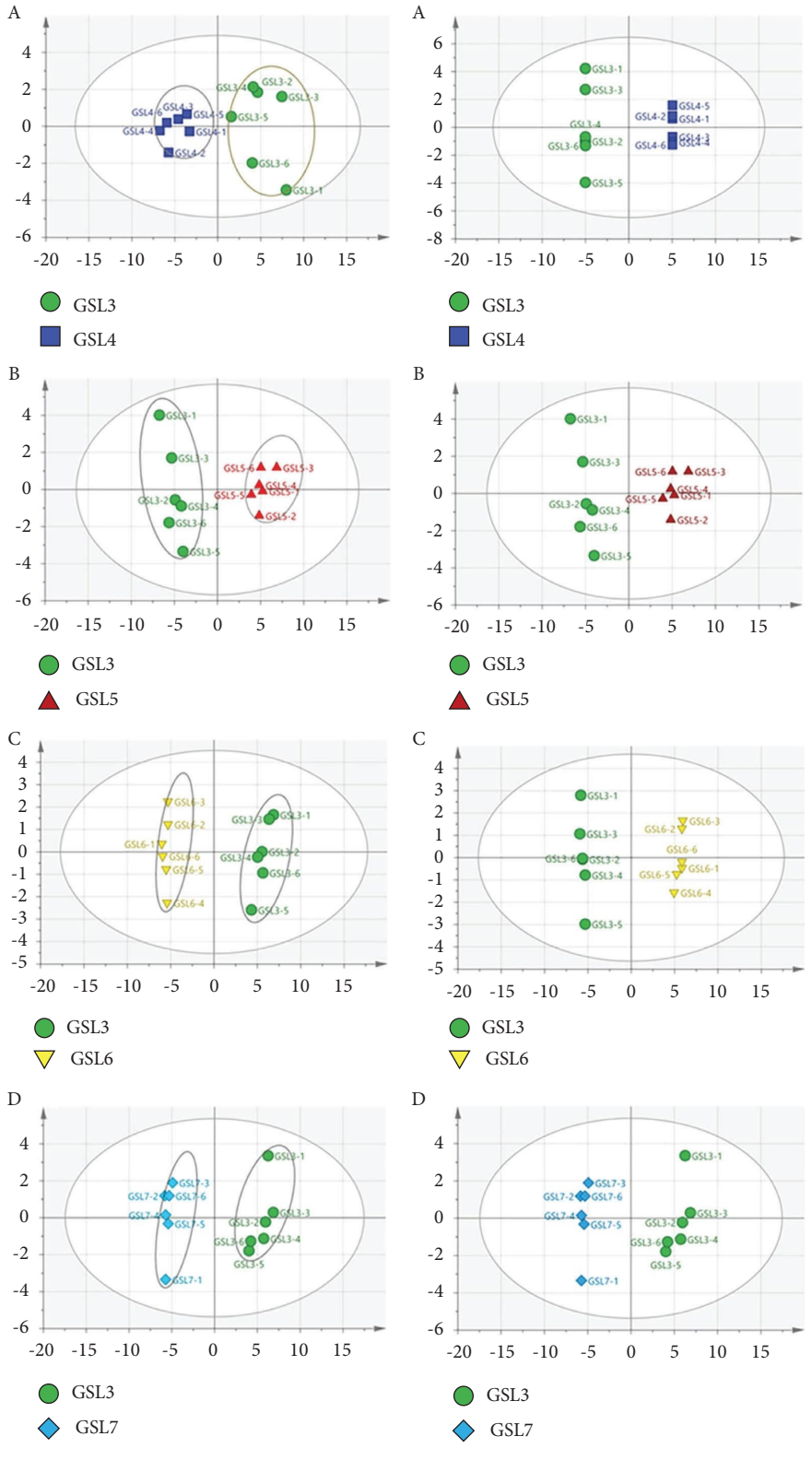

Figure 3: Score plots of PCA analysis (a) and OPLS-DA analysis (b) of GSL3 vs. GSL4 (A), GSL3 vs. GSL5 (B), GSL3 vs. GSL6 (C), and GSL3 vs. GSL7 (D).

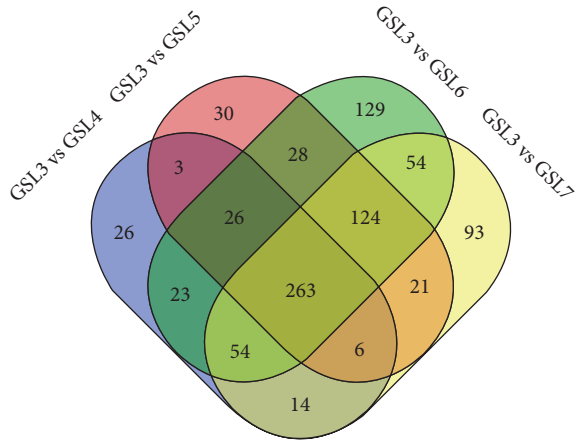

Figure 4: Venn diagrams of the number of different compounds of GSL from 3-, 4-, 5-, 6-, and 7-year-olds.

value. As a result, 32 metabolites were selected to be identified, and fold change values were also conducted to express the variation trends between the four compared groups (Table 1). According to reports, the target volatile components were mainly terpenes, alcohols, acids, esters, aldehydes, and alkanes [37]. Terpenoids are the largest group of natural products discovered in plants. Sesquiterpenes, the largest subgroup of terpenoids, are known as more than 7,000 species components and possessed many functions in plant physiological and ecological interactions [38–40]. Plants produce sesquiterpenes as bioactive compounds to protect themselves from insects and pathogenic microorganisms [41]. Sesquiterpenes have shown to contribute to defense in multiple plant species [42]. Figure 5 shows the identified volatile components labeled in TIC, profiles of intensities of 32 common differential compounds from GSLs revealing changes within various growth periods. The peak intensities of GSL 3 vs. 4, 5, 6, and 7 were all significantly different ($P < 0.05$) (Figure 6). Regarding specific compounds, differential compounds 1–3 (C1–C3) had the highest content in the GSL5 and showed irregular changes with the growth years; differential compound 4 (C4) had the highest content in the GSL4; the GSL3 had the highest concentration of differential compounds including C5, 16, and 21–24, 27, 30, and 32; and differential compounds 5, 21, and 24 and 30 (C5, 21, 24, and 30) showed a downward trend with age. Differential compounds 6–16 (C6–C16) and 17–20 (C17–C20) were the highest in GSL6. With GSL6 as the turning point, the content increased with the increase of years in GSL3–GSL6 years and decreased significantly in GSL7. The content of metabolites 25, 26, 28, 29, and 31 (C25–29 and C31) were the highest in GSL7 and decreased from GSL3 to GSL6. It should also be noted that the GSL4 showed a downward trend in the volatile components identified above and the GSL6 showed an upward trend in the volatile substances mentioned above, especially sesquiterpenes, indicating that the GSL6 may contain more volatile components than the GSL4. This result may provide a new direction for the identification of GSL in different growth years.

A heatmap was generated using those 32 metabolites gained above by MetaboAnalyst 5.0 (Figure 7(a)). In order to find out the metabolites that contribute to age prediction obtained from OPLS-DA result, with the significant value of VIP >1 and P value <0.05 as the screening standard of potential biomarkers, 32 metabolites between the four compared groups (GSL3 vs. 4, 5, 6, and 7) were analyzed to determine the most valuable potential biomarkers. The fluctuation trend and intensity changes between different metabolites can be obtained by correlation heatmap analysis and statistical histogram of the differential metabolites (Figures 7(b) and 7(c)). For the purpose of evaluating the biomarker that contributed to prominent age discrimination capacity, the receiver operating characteristic (ROC) analysis was employed for all data of four compared model groups. The area under the curve (AUC) value was used to show the extent of deviation between 3- and 4-, 3-and 5-, 3- and 6-, and 3- and 7-year-old GSL, respectively. In our results, 32 metabolites previously identified all gain good value (AUC value >0.8) on the contribution of age discrimination (Tables S1 to S4). Significantly, the metabolite named 1-Cyclohexene-1-carboxaldehyde, 2, 6, 6-trimethyl- showed an excellent prediction with the AUC value of 1.0 among all the four compared groups (Figure 7(d)), which also demonstrated that it could be the potential biomarker to discriminate the 3- and 5-, 3- and 6-, and 3- and 7-year-old GSL. The observation showed a significant effect on the chemical composition of GSLs influenced by cultivation years, especially on the VOCs.

Polysaccharides, proteins, and ginsenosides are the key and dominating ingredients in ginseng plants, which are responsible for structural formation, energy reserves, and physiological accommodation [43–45]. In this study, the contents of crude polysaccharides, total protein, and total ginsenosides are shown to be irregular changes with the growth age increased. The current results provided an indication of GSLs application on specific compositions. If the polysaccharides and proteins are selected as the research objects, 4-year-old GSLs will be a good choice. If the studied objects are the saponins, it is better to choose 3-year-old GSLs. If volatile oil is going to be the target, it is recommended to harvest the 6-year-old GSLs.

Table 1: Identification of common differential compounds of GSLs with the cultivation years 3–7.

No.	t (min)	Formula	RIx	RI	Identification	Fold change							
						GSL4 vs. 3	Trends	GSL5 vs. 3	Trends	GSL6 vs. 3	Trends	GSL7 vs. 3	Trends
1	4.48	$C_6H_{10}O$	832.14	832	2-Hexenal	−0.4173	↓	−0.7684	↓	−0.2313	↓	0.66097	↑
2	4.52	$C_8H_{14}O_3$	834.52	833	2-Hexenal, (E)-	−0.5939	↓	−0.4313	↓	1.1642	↑	−5.7134	↓
3	4.76	$C_6H_{12}O$	848.81	845	3-Hexen-1-ol	−0.3425	↓	−0.2809	↓	1.28703	↑	0.27624	↑
4	7.28	$C_8H_{16}O$	994.86	995	Octanal	0.23339	↑	0.79992	↑	2.08758	↑	−3.4447	↓
5	9.15	$C_9H_{18}O$	1106.41	1107	Nonanal	−0.3755	↓	−0.9359	↓	1.20856	↑	−4.6067	↓
6	10.9	$C_{10}H_{16}$	1219.86	1219	1-Cyclohexene-1-carboxaldehyde, 2,6,6-trimethyl-	0.01689	↑	0.79479	↑	3.19713	↑	3.28437	↑
7	13.34	$C_{15}H_{24}$	1392.7	1393	Cyclohexane,1-ethenyl-1-methyl-2,4-bis(1-methylethenyl)-, [1S-(1α,2β,4β)]-	−0.1963	↓	0.8731	↑	1.9101	↑	−0.706	↓
8	13.38	$C_{15}H_{24}$	1395.62	1397	γ-Elemene	−0.4119	↓	0.98547	↑	1.97849	↑	0.84634	↑
9	13.73	$C_{15}H_{24}$	1422.48	1423	Tricyclo[2.2.1.0(2,6)]heptane,1,7-dimethyl-7-(4-methyl-3-pentenyl)-, (-)-	−0.3977	↓	0.72522	↑	−1.5615	↓	3.13969	↑
10	13.9	$C_{15}H_{24}$	1435.66	1435	Bicyclo[2.2.1]heptane,2-methyl-3-methylene-2-(4-methyl-3-pentenyl)-, (1S-endo)-	−0.5645	↓	1.112	↑	1.18175	↑	−0.424	↓
11	14.09	C_8H_{10}	1450.39	1450	(E)-β-Farnesene	−0.3332	↓	1.03452	↑	2.27293	↑	−3.4411	↓
12	14.26	$C_{15}H_{24}$	1463.57	1462	α-Farnesene	−0.3393	↓	0.50874	↑	1.14356	↑	−3.7874	↓
13	14.33	$C_{15}H_{24}$	1468.99	1468	Alloaromadendrene	−0.6932	↓	0.23713	↑	2.11348	↑	−1.3898	↓
14	14.47	$C_{15}H_{24}$	1479.84	1476	Spiro[4.5]dec-7-ene,1,8-dimethyl-4-(1-methylethenyl)-,[1S-(1π4π5π]-	−0.5067	↓	0.56542	↑	2.12905	↑	0.70809	↑
15	14.57	$C_{15}H_{24}$	1487.6	1485	1,6-Cyclodecadiene,1-methyl-5-methylene-8-(1-methylethyl)-,[S-(E,E)]-	−0.4456	↓	1.44055	↑	1.85713	↑	2.04415	↑
16	14.68	$C_{13}H_{20}O$	1496.12	1496	3-Buten-2-one,4-(2,6,6-trimethyl-1-cyclohexen-1-yl)-	−0.4164	↓	1.06994	↑	1.1758	↑	−0.6165	↓
17	14.7	$C_{15}H_{24}$	1497.67	1497	Naphthalene,1,2,3,4,4a,5,6,8a-octahydro-4a,8-dimethyl-2-(1-methylethenyl)-,[2R-(2α,4aα,8aβ)]-	−0.5278	↓	1.55448	↑	−0.0697	↓	−0.2368	↓
18	14.73	$C_{15}H_{32}$	1500	1500	Pentadecane	−0.5662	↓	0.57197	↑	1.95523	↑	0.02009	↑
19	14.78	$C_{15}H_{24}$	1504.1	1502	Naphthalene,1,2,4a,5,6,8a-hexahydro-4,7-dimethyl-1-(1-methylethyl)-	−0.8071	↓	0.74587	↑	1.39404	↑	−1.1603	↓
20	14.93	$C_{15}H_{24}$	1516.39	1513	(+)-Valencene	−0.452	↓	0.35627	↑	1.75483	↑	1.15871	↑
21	14.95	$C_{11}H_{16}O_2$	1518.03	1520	2(4H)-Benzofuranone,5,6,7,7a-tetrahydro-4,4,7a-trimethyl-, (R)-	−0.4897	↓	−0.1801	↓	−2.5388	↓	−2.2159	↓
22	15.47	$C_{15}H_{26}O$	1560.66	1559	1,6,10-Dodecatrien-3-ol, 3,7,11-trimethyl-	−0.5177	↓	0.07881	↑	−1.6998	↓	−5.8015	↓
23	15.55	$C_{16}H_{34}$	1567.21	1570	Pentadecane, 3-methyl-	−0.6434	↓	0.99403	↑	3.41088	↑	2.65057	↑
24	15.74	$C_{15}H_{24}O$	1582.79	1584	1H-Cycloprop[e] azulen-7-ol,decahydro-1,1,7-trimethyl-4-methylene-,[1ar-(1aα,4aα,7β,7aβ,7bα)]-	−0.5835	↓	−0.3625	↓	0.77657	↑	−4.1101	↓
25	15.78	$C_{15}H_{26}O$	1586.07	1587	1H-Cycloprop[e]azulen-4-ol, decahydro-1,1,4,7-tetramethyl-, [1aR-(1aπ4π4aπ7π7aπ7bπ]-	−0.3069	↓	0.32129	↑	1.80712	↑	−4.8364	↓
26	15.9	$C_{15}H_{26}O$	1595.9	1595	Ledol	−0.2061	↓	0.06467	↑	1.80252	↑	−1.2078	↓
27	15.98	$C_{16}H_{34}$	1602.56	1600	Hexadecane	−0.9242	↓	−0.7128	↓	0.37984	↑	0.94954	↑
28	16.29	$C_{15}H_{24}O$	1629.06	1624	α-Santalol	0.61358	↑	−0.128	↓	0.46372	↑	0.86582	↑
29	16.75	$C_{15}H_{24}O$	1668.38	1668	β-Santalol	−0.2857	↓	0.34556	↑	−0.9167	↓	0.58392	↑
30	16.83	$C_{15}H_{24}O$	1675.21	1672	Aromadendrene oxide-(1)	−1.0618	↓	1.5634	↑	1.02732	↑	−0.4852	↓
31	16.85	$C_{15}H_{24}O$	1676.92	1678	Aromadendrene oxide-(2)	−1.4179	↓	1.85217	↑	3.10534	↑	−1.6804	↓
32	17.10	$C_{17}H_{36}$	1698.29	1700	Heptadecane	−1.4769	↓	1.11836	↑	3.17258	↑	−0.5075	↓

Trends "↑" means upregulation and "↓" means downregulation.

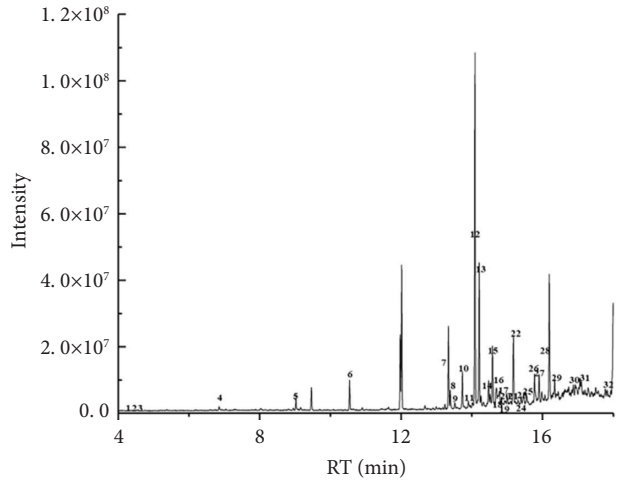

Figure 5: The total ion chromatogram (TIC) of the 32 identified common differential compounds. (Note: numbers 1–32 represent 32 identified common differential compounds by NIST 11 in GSLs.)

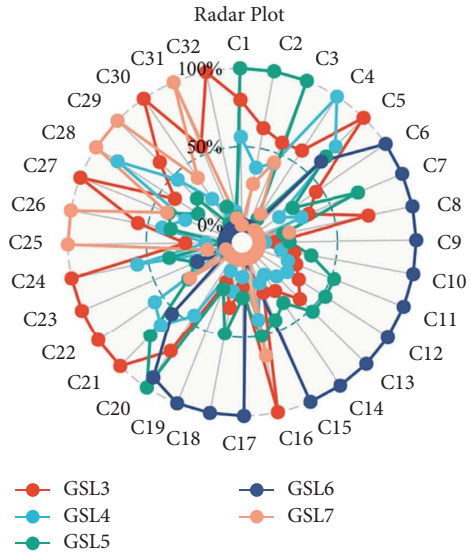

Figure 6: Profiles of 32 common differential compounds (compound 1–32 and C1–C32) from GSLs revealing changes in intensities within various harvest periods. The peak intensities of GSL 3 vs. 4, 5, 6, and 7 were all significantly different ($P < 0.05$).

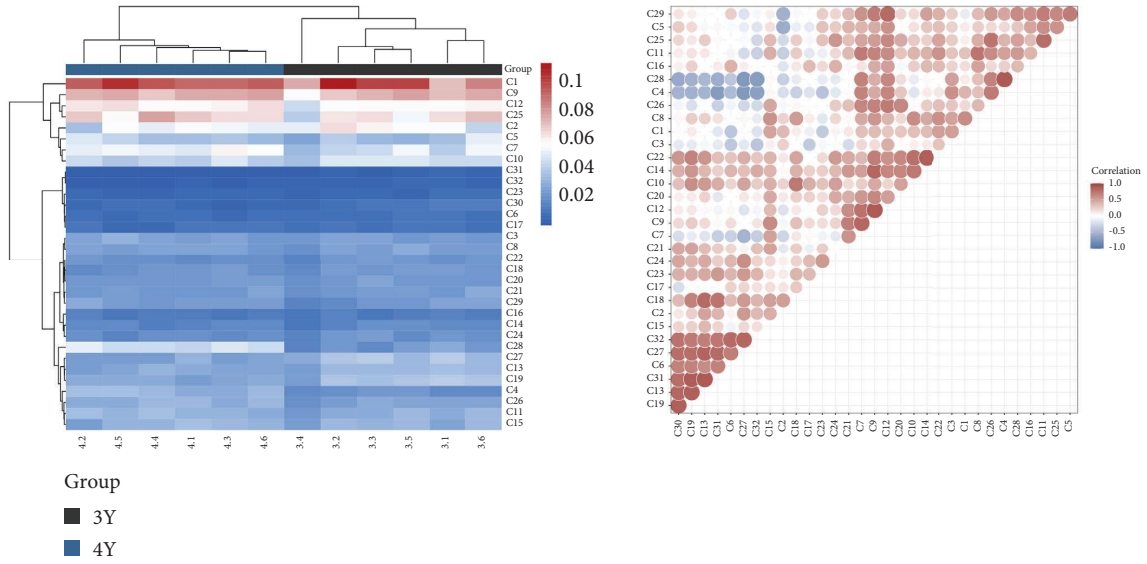

(a) (b)

Figure 7: Continued.

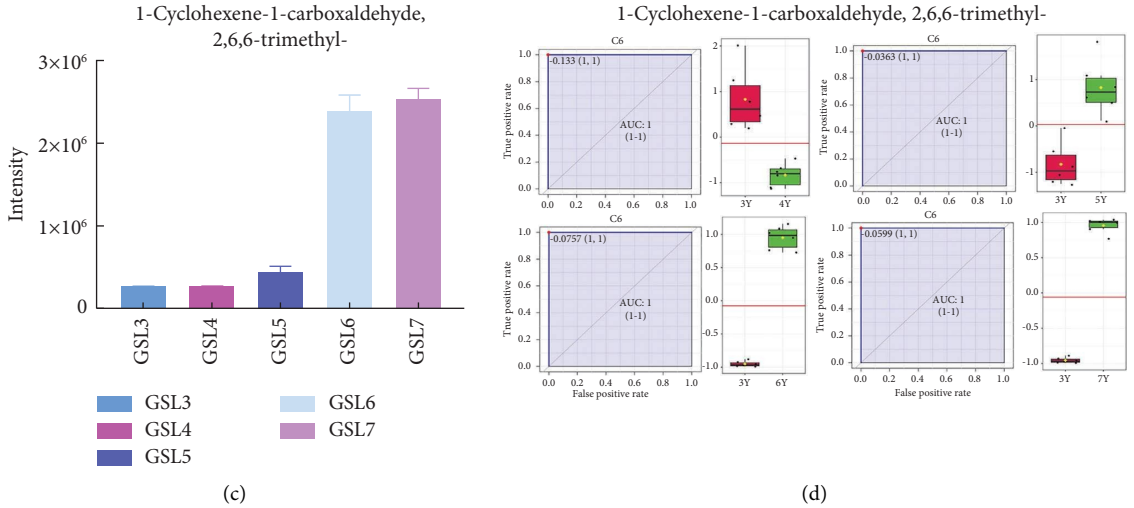

Figure 7: Potential biomarker analysis: (a) the identified differential metabolite heatmap between GSL3 and GSL4 horizontally represent each sample in the two groups and longitudinally represent the differential metabolites in each sample. (b) Correlation heatmap of the differential metabolites among GSL3 and GSL4; red means positive correlation and green means negative correlation. (c) Intensity changes of 1-cyclohexene-1-carboxaldehyde, 2, 6, 6-trimethyl- from GSL3 to GSL7. (d) AUC curve of 1-cyclohexene-1-carboxaldehyde, 2, 6, 6-trimethyl-.

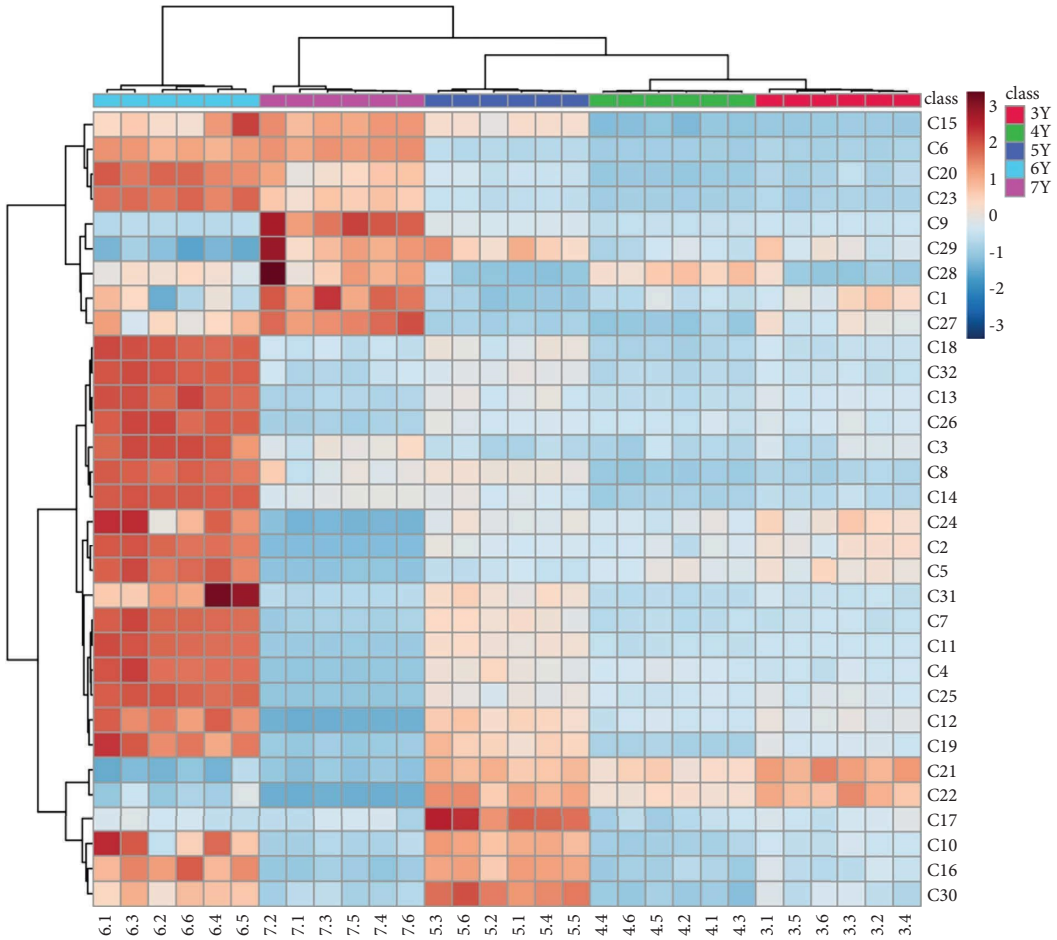

Figure 8: Hierarchical cluster analysis of the 3–7 year ginseng stems and leaves based on their volatile compounds. Note: ginseng stems and leaves on the 3rd year (3.1, 3.2, 3.3, 3.4, 3.5, and 3.6), on the 4th year (4.1, 4.2, 4.3, 4.4, 4.5, 4.6), on the 5 th year (5.1, 5.2, 5.3, 5.4, 5.5, and 5.6), on the 6th year (6.1, 6.2, 6.3, 6.4, 6.5, and 6.6), and on the 7th year (7.1, 7.2, 7.3, 7.4, 7.5, and 7.6).

3.6. HCA of HS-SPME-GC-MS Analysis. The 32 kinds of volatile compounds were the elements of this new data matrix, and the matrix with dimensions of 5 samples × 6 parallel replicates × 32 variables (volatiles) was constructed to perform HCA (Figure 8). These classification groups were consistent with the PCA results. In addition, six replicate samples at each harvest age were closely related, which further proved the great repeatability within the group. Therefore, it could be speculated that the GC-MS is highly correlated in distinguishing the volatile compound changes of ginseng stems and leaves during the different harvest periods, which could be confirmed by PCA and HCA. In conclusion, the HS-SPME combined with GC-MS was applied to the analysis of 3–7 year ginseng stems and leaves, and it was highly efficient and meaningful in the volatile components' research.

4. Conclusions

In this study, dynamic variations in the volatile composition of GSLs of five growth periods were investigated by using HS-SPME-GC-MS, combined with untargeted metabolomics analysis. A total of 263 active volatile metabolites were identified, among which 32 volatile metabolites were identified as critical volatile metabolites for discriminating the 3- and 4-, 3- and 5-, 3- and 6-, and 3- and 7-year-old GSL, but not all the compared groups. Notably, there was one volatile component of sesquiterpenes, which are the unique constitutions in ginseng and could be the potential biomarker to discriminate all the compared groups including the 3- and 4-, 3-and 5-, 3- and 6-, and 3- and 7-year-old GSL. The results could provide a basis for the determination of the harvesting time of GSLs and the study of factors causing the difference in quality. Overall, our findings provided new insights into variations in the volatile metabolite profiles of GSLs during different growth ages and improved our understanding of the chemical nature of the characteristics of different growth periods of GSLs.

Data Availability

The data used to support the findings of this study are included within the article.

Conflicts of Interest

The authors declare that they have no conflicts of interest.

Acknowledgments

This work was sponsored by the Jilin Province Science and Technology Development Plan Project (Grant nos. 20200404042YY and 20210401108YY), the National Natural Science Foundation of China (Grant no. 82073969), the key technology research project of Changchun Science and Technology Bureau (Grno. 21ZGY10), and Jiayi Biochemical Research and Development Center (Suzhou Industrial Park) Co., Ltd.

Supplementary Materials

We had one supplementary file. Tables S1–S4 are used to demonstrate the AUC values among the GLS with various growth ages. (*Supplementary Materials*)

References

[1] S. J. Kim, J. Y. Jang, and E. J. Kim, "Ginsenoside Rg3 restores hepatitis C virus-induced aberrant mitochondrial dynamics and inhibits virus propagation," *Hepatology*, vol. 66, pp. 758–771, 2017.

[2] M. Y. Liu, Y. P. Ren, L. J. Zhang, and J. Y. Ding, "Pretreatment with Ginseng fruit saponins affects serotonin expression in an experimental comorbidity model of myocardial infarction and depression," *Aging Dis*, vol. 7, pp. 680–686, 2016.

[3] Y. S. Wang, H. Li, Y. Li, H. Zhu, and Y. H. Jin, "Identification of natural compounds targeting annexin A2 with an anticancer effect," *Protein Cell*, vol. 9, no. 6, pp. 568–579, 2018.

[4] D. Yoon, B. R. Choi, S. Ma et al., "Metabolomics for age discrimination of ginseng using a multiplex approach to HR-MAS NMR spectroscopy, UPLC-QTOF/MS, and GC × GC-TOF/MS," *Molecules*, vol. 24, no. 13, p. 2381, 2019.

[5] Y. Wang, J. J. Zhang, J. G. Hou et al., "Protective effect of ginsenosides from stems and leaves of Panax ginseng against scopolamine-induced memory damage via multiple molecular mechanisms," *American Journal of Chinese Medicine*, vol. 50, no. 04, pp. 1113–1131, 2022.

[6] Z. E. Jimenez Perez, R. Mathiyalagan, J. Markus et al., "Ginseng-berry-mediated gold and silver nanoparticle synthesis and evaluation of their in vitro antioxidant, antimicrobial, and cytotoxicity effects on human dermal fibroblast and murine melanoma skin cell lines," *International Journal of Nanomedicine*, vol. 12, pp. 709–723, 2017.

[7] W. Liu, J. Leng, J. G. Hou et al., "Saponins derived from the stems and leaves of*Panax ginseng*attenuate scrotal heat-induced spermatogenic damage via inhibiting theMAPKmediated oxidative stress and apoptosis in mice," *Phytotherapy Research*, vol. 35, no. 1, pp. 311–323, 2021.

[8] F. Pu, C. M. Alfaro, V. Pirro, Z. Xie, Z. Ouyang, and R. G. Cooks, "Rapid determination of isocitrate dehydrogenase mutation status of human gliomas by extraction nanoelectrospray using a miniature mass spectrometer," *Analytical and Bioanalytical Chemistry*, vol. 411, no. 8, pp. 1503–1508, 2019.

[9] C. Zhang, N. Kong, M. Cao, D. Wang, Y. Chen, and Q. Chen, "Evolutionary significance of amino acid permease transporters in 17 plants from chlorophyta to angiospermae," *BMC Genomics*, vol. 21, no. 1, p. 391, 2020.

[10] R. Ghan, J. Petereit, R. L. Tillett et al., "The common transcriptional subnetworks of the grape berry skin in the late stages of ripening," *BMC Plant Biology*, vol. 17, no. 1, p. 94, 2017.

[11] E. Stahl, M. Hartmann, N. Scholten, and J. Zeier, "A role for tocopherol biosynthesis in arabidopsis basal immunity to bacterial infection," *Plant Physiology*, vol. 181, no. 3, pp. 1008–1028, 2019.

[12] R. P. McQuinn, N. E. Gapper, A. G. Gray et al., "Manipulation of ZDS in tomato exposes carotenoid- and ABA-specific effects on fruit development and ripening," *Plant Biotechnology Journal*, vol. 18, no. 11, pp. 2210–2224, 2020.

[13] X. Chen, J. Li, X. Wang et al., "Full-length transcriptome sequencing and methyl jasmonate-induced expression profile analysis of genes related to patchoulol biosynthesis and

regulation in Pogostemon cablin," *BMC Plant Biology*, vol. 19, no. 1, p. 266, 2019.

[14] I. M. Chung, J. W. Kim, P. Seguin, Y. M. Jun, and S. H. Kim, "Ginsenosides and phenolics in fresh and processed Korean ginseng (Panax ginseng CAMeyer): effects of cultivation location, year, and storage period," *Food Chemistry*, vol. 130, no. 1, pp. 73–83, 2012.

[15] I. M. Chung, J. J. Lim, M. S. Ahn, H. N. Jeong, T. J. An, and S. H. Kim, "Comparative phenolic compound profiles and antioxidative activity of the fruit, leaves, and roots of Korean ginseng (Panax ginseng Meyer) according to cultivation yearsfiles and antioxidative activity of the fruit, leaves, and roots of Korean ginseng (Panax ginseng Meyer) according to cultivation years," *Journal of Ginseng Research*, vol. 40, no. 1, pp. 68–75, 2016.

[16] Y. Qu, T. Qiao, and Z. X. Zhou, "Determination of appearance morphology and content of 7 main ginsenosides of mountain ginseng under different ages of Shizhu forest," *Chinese Journal of Traditional Chinese Medicine*, vol. 32, pp. 2198–2200, 2014.

[17] N. Kim, K. Kim, B. Y. Choi et al., "Metabolomic approach for age discrimination of Panax ginseng using UPLC-Q-tof MS," *Journal of Agricultural and Food Chemistry*, vol. 59, no. 19, pp. 10435–10441, 2011.

[18] T. Dan, W. Ren, Y. Liu et al., "Volatile flavor compounds profile and fermentation characteristics of milk fermented by lactobacillus delbrueckii subsp. Bulgaricus," *Frontiers in Microbiology*, vol. 10, p. 2183, 2019.

[19] M. A. Farag and D. M. El-Kersh, "Volatiles profiling in Ceratonia siliqua (Carob bean) from Egypt and in response to roasting as analyzed via solid-phase microextraction coupled to chemometrics," *Journal of Advanced Research*, vol. 8, no. 4, pp. 379–385, 2017.

[20] W. A. Khan, M. B. Arain, Y. Yamini et al., "Hollow fiber-based liquid phase microextraction followed by analytical instrumental techniques for quantitative analysis of heavy metal ions and pharmaceuticals," *Journal of Pharmaceutical Analysis*, vol. 10, no. 2, pp. 109–122, 2020.

[21] H. Bagheri, H. Piri-Moghadam, and M. Naderi, "Towards greater mechanical, thermal and chemical stability in solid-phase microextraction," *TrAC, Trends in Analytical Chemistry*, vol. 34, pp. 126–139, 2012.

[22] B. A. McKenzie, J. Robles-Najar, E. Duong, P. Brisk, and W. H. Grover, "Chronoprints: identifying samples by visualizing how they change over space and time," *ACS Central Science*, vol. 5, no. 4, pp. 589–598, 2019.

[23] D. Stettin, R. X. Poulin, and G. Pohnert, "Metabolomics benefits from orbitrap GC-MS-comparison of low- and high-resolution GC-MS," *Metabolites*, vol. 10, no. 4, p. 143, 2020.

[24] S. Qi, L. Zha, Y. Peng et al., "Quality and metabolomics analysis of houttuynia cordata based on HS-SPME/GC-MS," *Molecules*, vol. 27, no. 12, p. 3921, 2022.

[25] W. Xu, A. van Knegsel, E. Saccenti, R. van Hoeij, B. Kemp, and J. Vervoort, "Metabolomics of milk reflects a negative energy balance in cows," *Journal of Proteome Research*, vol. 19, no. 8, pp. 2942–2949, 2020.

[26] A. K. Singh, S. Yadav, B. S. Chauhan et al., "Classification of clinical isolates of klebsiella pneumoniae based on their in vitro biofilm forming capabilities and elucidation of the biofilm matrix chemistry with special reference to the protein content," *Frontiers in Microbiology*, vol. 10, p. 669, 2019.

[27] W. N. Reichelt, D. Waldschitz, C. Herwig, and L. Neutsch, "Bioprocess monitoring: minimizing sample matrix effects for total protein quantification with bicinchoninic acid assay," *Journal of Industrial Microbiology and Biotechnology*, vol. 43, no. 9, pp. 1271–1280, 2016.

[28] S. Azzi-Achkouty, N. Estephan, N. Ouaini, and D. N. Rutledge, "Headspace solid-phase microextraction for wine volatile analysis," *Critical Reviews in Food Science and Nutrition*, vol. 57, no. 10, pp. 2009–2020, 2017.

[29] J. Hou, L. Liang, and Y. Wang, "Volatile composition changes in navel orange at different growth stages by HS-SPME-GC-MS," *Food Research International*, vol. 136, Article ID 109333, 2020.

[30] M. Jimenez, A. P. Guzman, E. Azuara, O. Garcia, M. R. Mendoza, and C. I. Beristain, "Volatile compounds and antioxidative activity of Porophyllum tagetoides extracts," *Plant Foods for Human Nutrition*, vol. 67, no. 1, pp. 57–63, 2012.

[31] G. Zhou, G. Xu, J. Hao, S. Chen, J. Xu, and X. Zheng, "Generalized centered 2-D principal component analysis," *IEEE Transactions on Cybernetics*, vol. 51, no. 3, pp. 1666–1677, 2021.

[32] B. Gelen and G. Guclu, "Comparison of volatile compounds in sesame oil and sesame cake extract," *Journal of Raw Materials to Processed Foods*, vol. 2, pp. 34-35, 2021.

[33] S. Stewart, M. A. Ivy, and E. V. Anslyn, "The use of principal component analysis and discriminant analysis in differential sensing routines," *Chemical Society Reviews*, vol. 43, no. 1, pp. 70–84, 2014.

[34] K. Tanabe, C. Hayashi, T. Katahira, K. Sasaki, and K. Igami, "Multiblock metabolomics: an approach to elucidate whole-body metabolism with multiblock principal component analysis," *Computational and Structural Biotechnology Journal*, vol. 19, pp. 1956–1965, 2021.

[35] N. M. L. Simon, J. Kusakina, A. Fernandez-Lopez, A. Chembath, F. E. Belbin, and A. N. Dodd, "The energy-signaling hub SnRK1 is important for sucrose-induced hypocotyl elongation," *Plant Physiology*, vol. 176, pp. 1299–1310, 2018.

[36] Y. Li, H. Quan, L. Liang et al., "Nontargeted metabolomics reveals the discrimination of cyclocarya paliurus leaves brewed by different methods," *Food Research International*, vol. 142, Article ID 110221, 2021.

[37] S. Cui, J. Wu, J. Wang, and X. Wang, "Discrimination of American ginseng and Asian ginseng using electronic nose and gas chromatography-mass spectrometry coupled with chemometrics," *Journal of Ginseng Research*, vol. 41, no. 1, pp. 85–95, 2017.

[38] D. Hou, "Study on volatile components of aboveground parts of ginseng," *Journal of Anshan Normal University*, vol. 03, pp. 34–40, 1990.

[39] J. D. Rudolf, L. B. Dong, H. Cao et al., "Structure of the ent-copalyl diphosphate synthase PtmT2 from streptomyces platensis CB00739, a bacterial type II diterpene synthase," *Journal of the American Chemical Society*, vol. 138, no. 34, pp. 10905–10915, 2016.

[40] E. M. Bertrand, R. Keddis, J. T. Groves, C. Vetriani, and R. N. Austin, "Identity and mechanisms of alkane-oxidizing metalloenzymes from deep-sea hydrothermal vents," *Frontiers in Microbiology*, vol. 4, p. 109, 2013.

[41] M. C. Schuman, E. C. Palmer-Young, A. Schmidt, J. Gershenzon, and I. T. Baldwin, "Ectopic terpene synthase expression enhances sesquiterpene emission in Nicotiana attenuata without altering defense or development of transgenic plants or neighbors," *Plant Physiology*, vol. 166, no. 2, pp. 779–797, 2014.

[42] T. L. Delatte, G. Scaiola, J. Molenaar et al., "Engineering storage capacity for volatile sesquiterpenes in Nicotiana benthamiana leaves," *Plant Biotechnology Journal*, vol. 16, no. 12, pp. 1997–2006, 2018.

[43] J. Van Dingenen, L. De Milde, M. Vermeersch et al., "Chloroplasts are central players in sugar-induced leaf growth," *Plant Physiology*, vol. 171, no. 1, pp. 590–605, 2016.

[44] Y. Wan, M. Mao, D. Wan et al., "Identification of the WRKY gene family and functional analysis of two genes in Caragana intermedia," *BMC Plant Biology*, vol. 18, no. 1, p. 31, 2018.

[45] W. T. Yang, Y. Wang, Y. H. Shi et al., "Herbal compatibility of ginseng and rhubarb exerts synergistic neuroprotection in cerebral ischemia/reperfusion injury of rats," *Frontiers in Physiology*, vol. 10, p. 1174, 2019.